

We are IntechOpen, the world's leading publisher of Open Access books Built by scientists, for scientists

6,900

Open access books available

186,000

International authors and editors

200M

Downloads

Our authors are among the

154

Countries delivered to

TOP 1%

most cited scientists

12.2%

Contributors from top 500 universities



WEB OF SCIENCE™

Selection of our books indexed in the Book Citation Index
in Web of Science™ Core Collection (BKCI)

Interested in publishing with us?
Contact book.department@intechopen.com

Numbers displayed above are based on latest data collected.
For more information visit www.intechopen.com



MeV Electron Irradiation of Ion-Implanted Si-SiO₂ Structures

Sonia B. Kaschieva and Sergey N. Dmitriev

Additional information is available at the end of the chapter

<http://dx.doi.org/10.5772/67761>

Abstract

The effect of (10–25) MeV electron irradiation on Si-SiO₂ structures implanted with different ions (Ar, Si, O, B, and P) has been investigated by different methods, such as deep-level transient spectroscopy (DLTS), thermo-stimulated current (TSCM), Rutherford backscattering (RBS), and soft X-ray emission spectroscopy (SXES). It has been shown that in double-treated Si-SiO₂ structures, the defect generation by high-energy electrons depends significantly on the location of preliminary implanted ions relative to the Si-SiO₂ interface as well as on the type (n- or p-Si) of silicon wafer. SiO₂ surface roughness changes, induced by ion implantation and high-energy electron irradiation of Si-SiO₂ structures, are observed by the atomic force microscopy (AFM). Si nanoclusters in SiO₂ of ion-implanted Si-SiO₂ structures generated by MeV electron irradiation is also discussed.

Keywords: Si-SiO₂ structures, ion implantation, MeV electron irradiation, radiation defects, Si nanoclusters

1. Introduction

The method of ion implantation is being extensively used to create a controlled distribution of impurity concentration in a definite region of the semiconductor (in particular Si) heterostructures and integrated circuits. Advantages of the method include precise control of the implanted species depth and profile. A disadvantage of the method is the creation of a large number of defects due to the breaking of bonds between atoms in the SiO₂-Si interface and in a thin Si surface layer. Although the ion implantation of the semiconductor's structures is an essential part of microelectronics device technology, some of its shortcomings, such as the accompanying substantial radiation-induced defects, are still a matter of concern.

Today, the use of radiation, in particular high-energy (MeV) irradiation, has become a valuable laboratory tool enabling researchers to study the generation, evolution, and annealing of the radiation-induced defects in semiconductor devices. Special attention is devoted to the radiation defects generated by ion implantation and by subsequent high-energy (MeV) electron irradiation. The results are a product of the collaboration between the Institute of Solid State Physics (Bulgarian Academy of Sciences) and the Joint Institute for Nuclear Research (JINR) (Dubna), Russia.

2. MeV electron irradiation of B⁺ ion-implanted Si-SiO₂ structures

The effect of a 12 MeV electron irradiation on Si-SiO₂ structures implanted with 50 keV boron ions (at $1.5 \times 10^{12} \text{ cm}^{-2}$) is studied by deep-level transient spectroscopy (DLTS) measurements. Metal Oxide Semiconductor (MOS) structures with oxide thickness 16.5 nm are used. B⁺ ions with energy of 50 keV and a dose of $1.5 \times 10^{12} \text{ ions/cm}^2$ were implanted through an SiO₂ layer. The ion energy induced the maximum damage well into the silicon matrix, about 120 nm away from the Si-SiO₂ interface. Al gate electrodes were then deposited using the photolithography technique. On the rear side (Ohm), Al contacts were deposited by thermal evaporation to form an MOS structure. The bombardment with 12 MeV electrons was completed from the gate side of the wafers. The irradiation was carried out on the MT-25 Microtron of the Flerov Laboratory of Nuclear Reactions at the JINR in Dubna, Russia. Each of the samples was irradiated for 10 or 60 s with a beam current from 5 to 6 μA . The sample holder was cooled during electron irradiation. **Figure 1** shows the DLTS spectra for MOS structures implanted with 50 keV boron ions (at $1.5 \times 10^{12} \text{ ions/cm}^2$) before and after the irradiation with 12 MeV electrons. The DLTS signal as a function of the sample temperature during the measurement is shown for different electron doses. **Figure 1(a)** corresponds to the as-implanted sample;

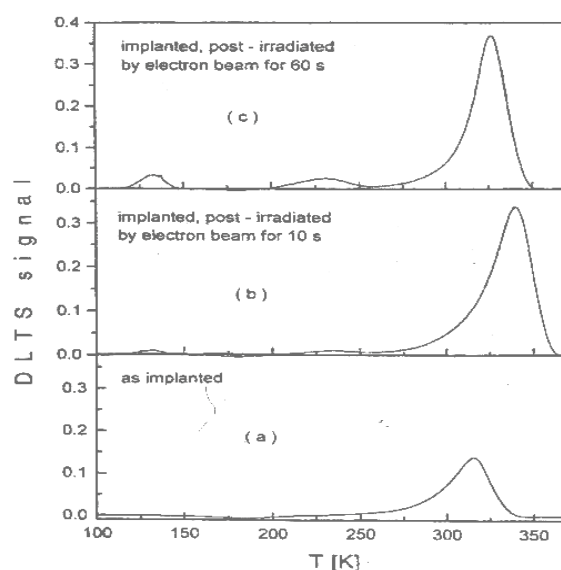


Figure 1. DLTS spectra for an Si-SiO₂ structure implanted with 50 keV B⁺ before (a) and after irradiation with 12 MeV electrons for 10 (b) and 60 s (c).

Figure 1(b) and **(c)** corresponds to the implanted wafers, which were post-irradiated with electrons for 10 and 60 s, respectively.

Additional shallow levels are found in the spectra after high-energy electron irradiation and the peak intensity being dependent on the irradiation dose. The parameters as activation energy of the defects, the density of traps, and the electron-capture cross-sections are evaluated.

According to **Figure 1(a)**, one kind of defects can be associated with the ion implantation, with a corresponding peak in the spectrum at about 320 K. In **Figure 1(b)** and **(c)** curves, this maximum increased along with two more peaks, located close to 135 K and 230 K. High-energy electrons create three different defect levels at $E_c - 0.21$, $E_c - 0.32$, and $E_c - 0.40$, which correspond to three distinct peaks of the DLTS spectra. The peak at $E_c - 0.40$ coincides with that of the DLTS spectrum for the as-implanted sample (**Figure 1a**). The density of all defects increases with the increase in electron irradiation doses. The trap density of the damage related to the implantation also increases after the electron bombardment. The concentration of the two new types of defects is increased lower than the increase in the concentration of those associated with ion implantation only.

The DLTS characteristic demonstrates that 50 keV boron ion implantation (at a dose of 1.2×10^{12} ions/cm²) creates mainly one kind of defect in the Metal Oxide Semiconductor (MOS) structures considered. These defects are located near the maximum of the ion-depth distribution, away from the Si-SiO₂ interface. High-energy irradiation by electrons enhances the contribution of such defects in the Si substrate and creates two additional states that are shallower on the energy scale. The DLTS measurements at different biases show that all states are most probably located at the Si-SiO₂ interface. The main level at $E_c - 0.40$ eV in the Si forbidden gap band can be attributed to the phosphorus-vacancy pair (P-V) or E center. $E_c - 0.21$ eV is related to di-vacancies and there are not enough data to relate the $E_c - 0.32$ eV level well enough to a specific type of defect [1].

The result suggests that the high-energy electrons generate the electrically active defects at the Si-SiO₂ interface of MOS structures more efficiently than in the silicon wafer.

3. MeV electron irradiation of O⁺, P⁺, or Si⁺-implanted Si-SiO₂ structures

In this work, we used Rutherford backscattering spectroscopy (RBS) in combination with channeling backscattering spectrometry (RBS/C). O⁺ or P⁺ and Si⁺ ion-implanted Si-SiO₂ structures irradiated with high-energy electrons have been studied.

n-type Si <100> oriented wafers oxidized at 1050°C in dry O₂ + 8% HCl ambient up to 22 nm were used. The Si-SiO₂ structures were implanted by P⁺ or O⁺ ions with an energy of 15 keV and a dose of 10¹² cm⁻². An ion beam energy of 15 keV was chosen so that the maximum number of implanted ions would be deposited close to or at the Si-SiO₂ interface. After implantation, both groups of implanted samples (with P⁺ or O⁺) were irradiated with different doses of 20 MeV electrons at a flux of about 10¹³ el/cm².s at room temperature. Three sets of samples were prepared from each of the two groups. The first set of Si-SiO₂ samples was implanted

by P^+ or O^+ ions, the second set of samples was implanted and then irradiated with 20 MeV electrons with a dose of $2.5 \times 10^{13} \text{ el/cm}^2$, and the third set was implanted and then irradiated with a dose of $1 \times 10^{15} \text{ el/cm}^2$.

Figure 2 shows that after both doses of electron irradiation, no significant changes in the RBS spectra of the samples are observed. The first peak of the RBS/C spectrum presents the oxygen concentration and the second one, the silicon concentration at the Si-SiO₂ interface of the sample. It is obvious that the two peaks appearing after the electron irradiation almost repeat the corresponding peaks of the as-implanted sample. Obviously, the silicon and oxygen distribution at the Si-SiO₂ interface in phosphorus-implanted Si-SiO₂ samples does not change after the electron irradiation. It is assumed that the low dose (10^{12} cm^{-2}) and the type of ion implantation (phosphorus) are the reasons for these negligible changes in the Si and O's peak height.

The RBS/C spectra of oxygen-implanted and electron-irradiated Si-SiO₂ samples are summarized in **Figure 3**. It shows that the silicon and oxygen peaks in the RBS/C spectrum of

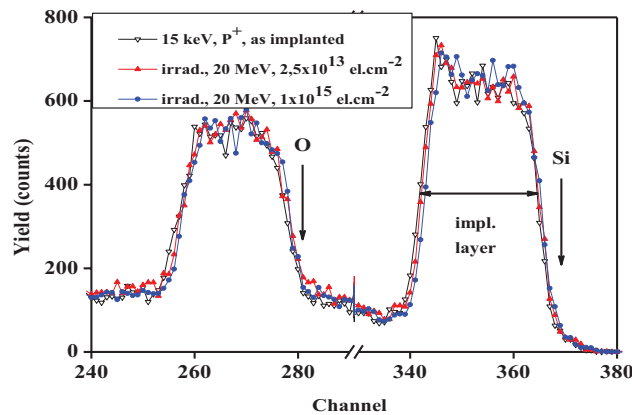


Figure 2. RBS spectra of P^+ -implanted n-Si-SiO₂ samples with a dose of 10^{12} cm^{-2} (curve 1) and MeV electron irradiated with doses of $2.5 \times 10^{13} \text{ el/cm}^2$ (curves 2) and $1 \times 10^{15} \text{ el/cm}^2$ (curves 3).

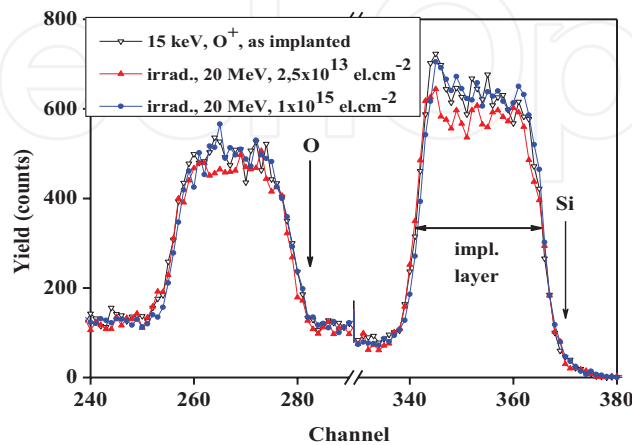


Figure 3. RBS spectra of n-Si-SiO₂ samples implanted by O^+ ions with a dose of 10^{12} cm^{-2} (curve 1) and MeV electron irradiated with doses of $2.5 \times 10^{13} \text{ el/cm}^2$ (curve 2) and $1 \times 10^{15} \text{ el/cm}^2$ (curve 3).

the oxygen-implanted samples increase after an MeV electron irradiation with a dose of 2.5×10^{13} el/cm² (curve 2). This increase is also observed after the second electron irradiation with a dose of 1×10^{15} el/cm² (curve 3). The increase of oxygen and silicon peaks' height (after high-energy electron irradiation) reveals an increase of silicon and oxygen concentrations in samples implanted with a low dose (10^{12} cm⁻²) of oxygen ions.

The results demonstrate that the same doses of electron irradiation result in an increase of both oxygen and silicon concentrations at the Si-SiO₂ interface of oxygen-implanted samples. Comparing the silicon peak's increase with that of the oxygen peak in the RBS/C spectra, one can conclude that the amount of silicon accumulated is larger than that of oxygen. It has been assumed that, along with the generation of radiation defects during electron irradiation, oxygen diffusion to the silicon substrate also takes place.

RBS spectra demonstrate that the MeV electron irradiation increases the oxygen and silicon concentrations in Si-SiO₂ samples implanted by O⁺ ions only [2].

4. MeV electron irradiation of Si⁺-implanted (with different doses) Si-SiO₂ structures

n-type Si <100> oriented wafers with a resistivity of 4.2 Ω cm were oxidized at 1000°C up to 36 nm. The samples were implanted with Si⁺ ions with an energy of 15 keV and a dose of 10^{12} cm⁻² or 10^{16} cm⁻². The energy of 15 keV was chosen so that the maximum number of the implanted ions would be deposited at the Si-SiO₂ interface. Both groups were irradiated with 20 MeV electrons for different durations (60 or 120 s). After the electron irradiation for 60 s, the RBS spectra of the sample remain unchanged. After 120 s of electron irradiation, the Si peak becomes wider to the left, and the peak corresponding to O atoms increases in the same way (about 11–12 Å). We assumed that the ion implantation defects, whose maximum is located close to the Si-SiO₂ interface, generate a thin layer of amorphous silicon at the silicon surface, close to the Si-SiO₂ interface. The subsequent electron irradiation generates additional radiation defects, which is the reason for the radiation-enhanced diffusion of oxygen and an insignificant increase of the amorphous layer's depth. Since after the electron irradiation both peaks of the RBS/C spectra (oxygen and silicon) widen in the same way, we can assume that during electron irradiation, the diffused oxygen penetrates the entire depth of the new amorphous silicon layer created by the additional electron irradiation.

RBS/C spectra of Si-SiO₂ samples implanted with Si⁺ ions with an energy of 15 keV and a dose of 10^{12} cm⁻² (curve B), which are electron irradiated for 60 (curves •) and 120 s (curves ■) are presented in **Figure 4a**. RBS/C spectra of Si-SiO₂ samples implanted with silicon ions at an energy of 15 keV and a dose of 10^{16} cm⁻² (curve B), which are electron irradiated for 60 (curves •) and 120 s (curves ■) and for 120 min (curve 0) are presented in **Figure 4b**.

The as-implanted sample exhibits an RBS spectrum similar to that in **Figure 5**. We assume that the amorphous silicon layer created by ion implantation appears only after the electron irradiation. The width increases as the ion implantation dose increases (10^{16} cm⁻²). The 60 or

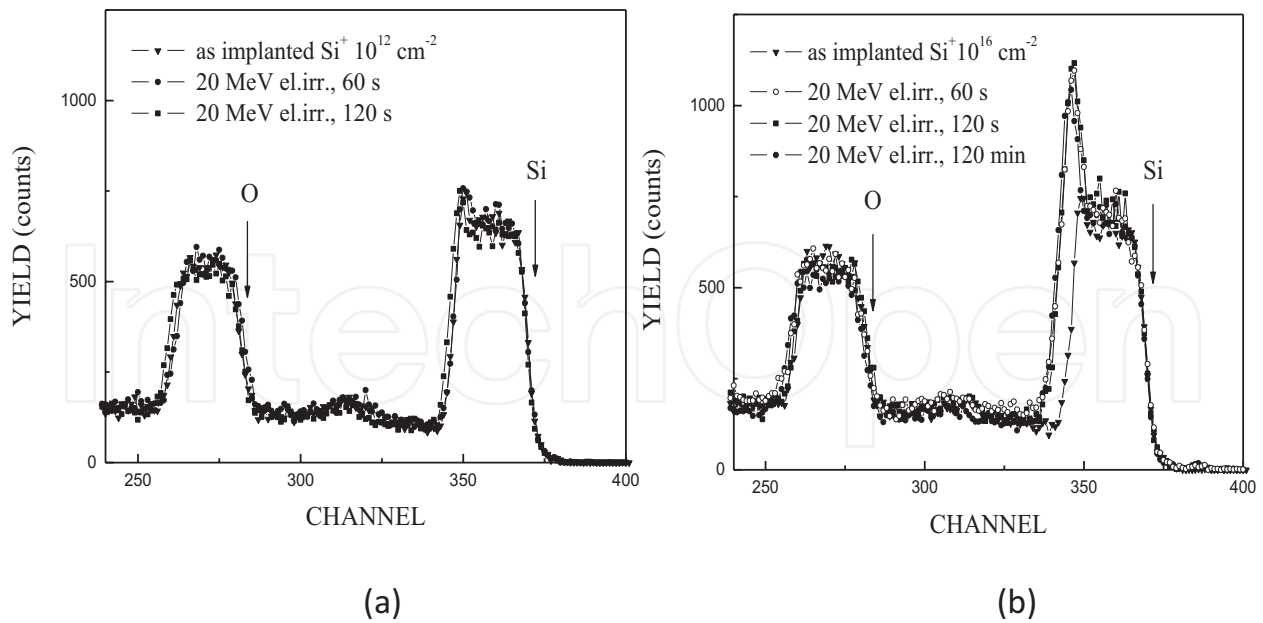


Figure 4. RBS/C spectra of Si-SiO₂ samples implanted with different doses Si⁺ ions (10¹² cm⁻²—(a)) and (10¹⁶ cm⁻²—(b)) which are 20 MeV electron irradiated.

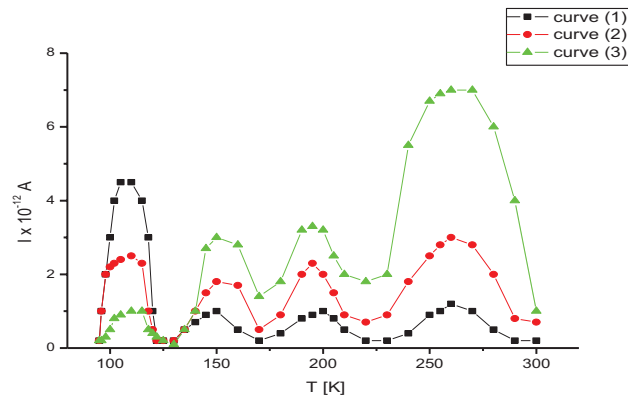


Figure 5. TSC spectra of only electron-irradiated MOS structures. Samples irradiated with doses of 1.2×10^{16} el/cm² (curve 1), 2.4×10^{16} el/cm² (curve 2), and 6.0×10^{16} el/cm² (curve 3).

120 s electron irradiation leads to the appearance of a new peak in the spectra. The creation of an additional amorphous silicon layer under the SiO₂ layer as a result of electron irradiation (6×10^{15} cm⁻²) is observed. After a 120-min electron irradiation, an additional widening of the main silicon peak in the RBS spectrum is observed to the left. The height of the oxygen peak decreases insignificantly, which means that an insignificant decrease of the oxygen concentration takes place. It is demonstrated that the amount of oxygen accumulated at the Si-SiO₂ interface is proportional to the decrease of the oxygen peak in the RBS/C spectrum. Along with the generation of radiation defects, oxygen diffusion to the amorphous layer is also observed during MeV electron irradiation. One can conclude that the widening of the amorphous layer is larger (about 47 Å) than the increase of the oxygen diffusion depth (which is about 12–13 Å). This indicates that during electron irradiation, only a fraction of the oxygen

is able to reach the amorphous silicon layer and remain there. Obviously, the defects created by electron radiation stimulate oxygen radiation-enhanced diffusion from the surface to the sample depth. We assume that only a part of the new amorphous layer created by electrons is a result of this diffusion. It is assumed that the shift of the oxygen peak in the RBS/C spectrum by one or two channels is demonstrated. The dramatic change in the Si profile after high-energy electron irradiation for 60 s is observed at the RBS/C spectra. This profile does not change significantly after the electron irradiation with twice as high a dose (after 120 s of irradiation). A small dose of electron irradiation is sufficient to create additional radiation defects and increase the amorphous silicon layer created by ion implantation. Obviously, the radiation defects created by the additional electron irradiation are not able to significantly increase this amorphous layer. We believe that the radiation defects induced by high-energy electron irradiation interact with those already created by a previous high dose of Si ion implantation, thus creating suitable conditions for an increase of the amorphous layer. The increase of the amorphous silicon layer is a result of the structural changes at the silicon surface created by the subsequent 20 MeV electron irradiation. We assume that a low dose of electron radiation is sufficient to create favorable conditions for an additional amorphization of the silicon surfaces. An additional increase of electron irradiation (up to 120 min) induces additional breaking of the strained bonds at the silicon surface. But the substantial energy deposited cannot significantly promote the amorphization process of the silicon wafer. In this case, the results show that the amorphization process depends more effectively on the Si implantation dose than on the electron irradiation dose [3].

5. MeV electron irradiation of Ar⁺-implanted Si-SiO₂ structures studied by TSC

The influence of 23 MeV electron irradiation (with doses of 1.2×10^{16} el/cm², 2.4×10^{16} el/cm², and 6.0×10^{16} el/cm² on the interface states of argon-implanted thin oxide Si-SiO₂ samples) has been studied by the thermally stimulated current (TSC) method. The samples are fabricated on n-Si wafers. The thermal oxidation is performed at 950°C to produce an oxide thickness of 18 nm. The samples are cooled in oxygen. Oxide thickness is measured by the ellipsometry method. Some of the Si-SiO₂ samples are implanted through the dioxide by 20 keV Ar⁺ ions with a dose of 5×10^{12} cm⁻². Energy of 20 keV is chosen so that the ions could penetrate through the oxide with a maximum damage production close to the Si-SiO₂ interface. Al gate electrodes are photolithographically defined. MOS capacitors are performed. The samples are simultaneously irradiated with 23 MeV electrons at a flux of about 2×10^{13} el/cm²s. Samples are irradiated at room temperature with doses of 1.2×10^{16} el/cm², 2.4×10^{16} el/cm², and 6.0×10^{16} el/cm², respectively.

The spectra reveal four peaks (at 120, 160, 195, and 260 K) corresponding to four kinds of energy states located at the Si-SiO₂ interface. Parameters of these interface states are determined by the initial rise plot and Grossweiner's methods. The interface states are associated with four discrete energy states in the Si band gap. Activation energy of traps is evaluated as: $E_c - 0.22$ eV, $E_c - 0.26$ eV, $E_c - 0.32$ eV, and $E_c - 0.45$ eV. The nature of defects corresponding to these traps is determined. There is a difference in the behavior of the first peak (which

reduces its height significantly) and the rest of the ones (which increase) during electron irradiation.

A decrease in height and area enclosed by the first peak is observed which means that the density of the defect (similar to acceptor level of the di-vacancies) decreases from 5.7 to $1.1 \times 10^{12} \text{ cm}^{-2}$ during irradiation. The area enclosed by deeper levels in the Si forbidden gap ($E_c - 0.26 \text{ eV}$, $E_c - 0.32 \text{ eV}$, and $E_c - 0.45 \text{ eV}$) increases with increasing electron dosage. The area enclosed by the last peak increases significantly from 3.9 up to $24 \times 10^{12} \text{ cm}^{-2}$. This peak of the spectra corresponding to the level $E_c - 0.45 \text{ eV}$ is associated with defects similar to vacancy-impurity complexes. They are the major kind of defects created by MeV electrons in silicon MOS structures.

The results show that Ar^+ implantation generates more kinds of defects at the Si-SiO₂ interface of MOS structures as compared to the defects generated by high-energy electron irradiation only.

Typical TSC curves for Ar^+ ion-implanted structures (curve 0), which are electron irradiated (curves 1–3), are shown in **Figure 6**. The spectra (which shift slightly to lower temperatures) are located at the temperature interval 80–200 K. Curve 0 presents as-implanted samples with 20 keV Ar^+ and a dose of $5 \times 10^{12} \text{ cm}^{-2}$. Ar^+ ions were used because inert gas ions have a low diffusion coefficient in the implanted layer and do not interact with Si. Ar ions form hard radiation defects only there, where (Si-SiO₂ interface in this case) they are located. Ion-implanted and electron-irradiated MOS samples with doses of $1.2 \times 10^{16} \text{ el/cm}^2$, $2.4 \times 10^{16} \text{ el/cm}^2$, and $6.0 \times 10^{16} \text{ el/cm}^2$ are presented by curves 1, 2, and 3, respectively. Thermal and field “cleaning” of the spectra is used. The last two peaks in the spectra of Ar-implanted samples (located at about 160 and 190 K) are clearly revealed after the electron irradiation. Energy positions of the five levels are determined by the initial rise plot and Grossweiner's methods. Curves 1–3 demonstrate that additional high-energy electron irradiation creates interface states, giving priority to deeper levels in the concentration which increases three to four times after irradiation. A considerable part of defects, induced by ion implantation, increase their concentration after increasing the electron radiation dose.

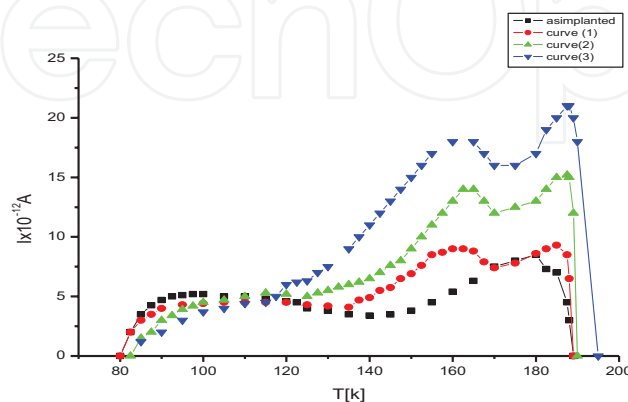


Figure 6. TSC curves for Ar^+ ion-implanted (curve 0) and electron-irradiated samples with doses of $1.2 \times 10^{16} \text{ el/cm}^2$, $2.4 \times 10^{16} \text{ el/cm}^2$, and $6.0 \times 10^{16} \text{ el/cm}^2$ (curves 1, 2, and 3, respectively).

When Ar ion-implanted structures are irradiated with the same doses of MeV electrons, the defects due to this irradiation interact in a different way with defects previously created by Ar ions. The concentration of defects like vacancy-oxygen and di-vacancy decreases slightly, and the concentration of vacancy-impurity complexes increases as the electron irradiation dose increases. We connect the shallow-level density decrease and deeper-levels density increase with the regrouping of collected simpler defects into more complicated ones. These results showed that the defects, which contain the basic impurity of a silicon wafer, determine the radiation defect generation at the Si-SiO₂ interface during high-energy electron irradiation. As a result of interaction between MeV electrons and an Ar ion-implanted MOS structure, the concentration of radiation defects (located at the Si-SiO₂ interface) changes in a different way (depending on their energy position in the Si band gap or on their nature). The concentration of shallow traps decreases slightly after the MeV electron irradiation. The concentration of deeper traps increases with electron irradiation's dose increasing.

The defects (generated by high-energy MeV electron irradiation), which contain the basic impurity of the Si wafer of MOS structures, determine the radiation defect concentration at the Si-SiO₂ interface (the best sensitivity part of the silicon MOS structure to the radiation) [4].

6. High-energy electron irradiation of ion-implanted Si-SiO₂ structures with different oxide thicknesses

The effects of 11 MeV electron irradiation of boron ion-implanted Si-SiO₂ structures with different oxide thicknesses have been investigated by the thermally stimulated charge (TSC) method. n-type <100> Si wafer samples are oxidized to different thicknesses of 11, 25, 54, 68, 105, and 120 nm and are implanted by 20 keV boron ions with a dose of $1.2 \times 10^{12} \text{ cm}^{-2}$. The ion energy and the oxide thickness of the samples are chosen so as to produce the maximum ion damage deep in the silicon substrate (for thinner oxide thickness), at the Si-SiO₂ interface (54 and 68 nm) and in the SiO₂ (for thicker oxides); Al gates are deposited onto the implanted surface of the wafers to form MOS structures. Thermally stimulated charge characteristics before and after the ion implantation or electron irradiation are measured in order to determine the parameters of the centers, induced by both treatments.

TSC spectra of 20 keV B⁺ implanted samples with different oxide thicknesses irradiated with 11 MeV electrons are shown in **Figure 7**. When ions are located deep in the Si matrix, mostly one kind of defect is induced and a peak at 175 K is observed. The energy positions of the corresponding traps are determined by the slope of the initial part of the peak and by the Grossweiner's method. They are in good agreement. $E_c - 0.40 \text{ eV}$ is the activation energy of these defects in the silicon forbidden gap. This center is attributed to the implantation. It is a lattice vacancy trapped at a substitutional phosphorus atom or phosphorus-vacancy pair (P-V) or "E" center. High-energy electron irradiation increases the density of these

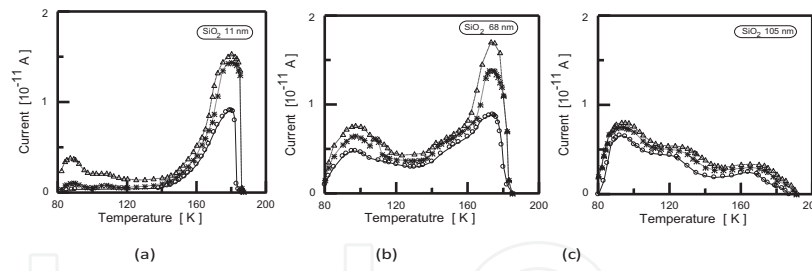


Figure 7. TSC spectra of 20 keV B⁺ ion-implanted samples with different oxide thicknesses (11 nm—**a**, 68 nm—**b**, and 105 nm—**c**) irradiated with 11 MeV electrons. As-implanted sample with a dose of $1.2 \times 10^{12} \text{ cm}^{-2}$ — curve 1—(o). Implanted and high-energy electron irradiated samples for 15, 30, and 60 s are represented by curves 2 (coinciding with curves 1—o), 3 (*), and 4 (Δ), respectively.

defects created by ion implantation ($E_c - 0.40 \text{ eV}$) and additionally generates two more kinds of defects. They are shallower on the energy scale in the Si forbidden gap: $E_c - 0.21 \text{ eV}$ and $E_c - 0.31 \text{ eV}$ (curves 3). The density of each of them increases as the electron irradiation dose increases.

When the maximum density of boron-implanted ions is located close to the Si-SiO₂ interface of the samples, several kinds of defects are created as can be seen in **Figure 7b**. The trap energies are determined by the initial rise method. They are $E_c - 0.16 \text{ eV}$, $E_c - 0.21 \text{ eV}$, $E_c - 0.25 \text{ eV}$, $E_c - 0.31 \text{ eV}$, and $E_c - 0.40 \text{ eV}$. The nature of these defects is also determinate: shallow-level $E_c - 0.16 \text{ eV}$ has been attributed to a vacancy trapped by an interstitial oxygen atom or “A” center. The next two levels $E_c - 0.21 \text{ eV}$ and $E_c - 0.25 \text{ eV}$ are correlated with double acceptor levels of di-vacancies. $E_c - 0.31 \text{ eV}$ and $E_c - 0.40 \text{ eV}$ —the last two kinds of traps—have already been discussed. In this case, the density of all levels related to the ion implantation increases with the following electron irradiation dose increasing. The density of the peaks located at 95 and 175 K (the dominant defects) increases more intensively. High-energy electron irradiation creates defects which can be associated mainly with vacancy-oxygen (A center) and vacancy-phosphorus (E center) complexes. The easier creation of interstitial atoms and vacancies near the ion-implantation complex defects are possible explanations of the intensive increase of their trap density. The process of radiation-induced defect formation as a result of both treatments is most active just in the surface region as the Si-SiO₂ interface is also a source of defect. In this case (**Figure 6b**, curves 3–4), the total density of the induced defects at the Si-SiO₂ interface (after the electron irradiation) is larger than in the case of first group samples, when the maximum damage as a result of the implanted ions is deep in the Si wafers (**Figure 6a**, curves 3–4) and in the case of third group samples (**Figure 6c**, curves 3–4), when the maximum of the implanted ions is in the SiO₂.

MeV electron irradiation of 20 keV boron ion-implanted structures generates defects, with a trap spectrum, which locates in the same temperature range as the spectrum of the as-implanted samples. After MeV electron irradiation, the density of radiation-induced interface traps depends on the disposition of the maximum of the previously implanted boron ions with respect to the Si-SiO₂ interface. The density of all levels related to the ion implantation increases uniformly with a dose increase of the following electron irradiation, in this case, when the maximum of the implantation-induced defects is located in the SiO₂ bulk.

It can be concluded that in the double treatment (B⁺ implantation plus MeV electron irradiation) of the Si-SiO₂ structures, the defect generation with high-energy electron irradiation significantly depends on the location of the preliminary implanted ions relative to the Si-SiO₂ interface [5].

7. A soft X-ray emission spectroscopy study of SiO₂/Si-implanted structures irradiated with MeV electrons

The investigations were carried out with two series of samples—n-Si and p-Si wafers—cut along the <100> crystallographic plane. Oxide layers with a thickness of 150 nm (for both series) were grown in dry oxygen at 1100°C. After oxidation, the samples were cooled at a rate of about 25°C/min, in the same ambient in which the oxidation is carried out. Then, some of the samples were implanted through the dioxide with Si⁺ ions, at an energy of 65 keV and a dose of $1.25 \times 10^{12} \text{ cm}^{-2}$.

Prior to implantation, half of each wafer was covered with a screen and was used for control measurements to compare its properties with those of the samples exposed to ion implantation or electron irradiation or both. After implantation, both series were irradiated with 20 MeV electrons at a flux of about $10^{13} \text{ el/cm}^2\text{-s}$, for different durations from 15 to 120 s. The Si L_{2,3} X-ray emission spectra were measured using an ultrasoft X-ray spectrometer of high spatial ($\Delta S \cdot 0.4 \text{ }\mu\text{m}$) and energy ($\Delta E \cdot 0.4 \text{ eV}$) resolution. An electron beam with an energy varying from 2 to 8 keV excited the spectra. The anode current was about 130 nA. The Si L_{2,3} X-ray emission spectra of SiO₂ (150 nm)/p-Si and (150 nm)/n-Si samples implanted with Si⁺ ions and then irradiated by 20 MeV electrons are shown in **Figure 8**. The spectra obtained at electron excitation energies of 2 and 4 keV are very similar to those of SiO₂. The spectra measured at 6 and 8 keV can be represented by a superposition of those of the reference specimens, SiO₂ and crystalline silicon (c-Si). The contributions of c-Si and SiO₂ to the 6 keV spectra are also shown in **Figure 8**.

Irradiation with 20 MeV electrons for 120 s leads to small increases in the SiO₂ contributions to the 6- and 8 keV spectra. The increase in the SiO₂ contribution is more pronounced for specimens prepared on n-type silicon wafers. This means that the high-energy electron irradiation leads to the oxidation of the SiO₂/Si samples. This oxidation effect is more prominent for the n-type Si samples. Preliminary implantation of the samples (with 65 keV Si⁺ ions) blocks the oxidation of the structures, as can be seen in **Figure 9**.

One can suggest that the oxide growth occurs due to additional number of oxygen atoms located at, or close to, the SiO₂/Si interface in the Si substrate. After irradiation, Si-Si bonds are broken. The number of oxygen atoms also increases. We show that the effect of radiation-stimulated oxidation (as a result of high-energy electron irradiation) is not strong for the SiO₂/Si samples cooled in the oxygen ambient after their thermal oxidation. We believe that a saturation of dangling bonds at the SiO₂/Si interface occurs during the post-oxidation cooling in the same ambient in which the thermal oxidation of samples was carried out. Saturation of the dangling bonds may be the reason for the increase in radiation hardness of the samples

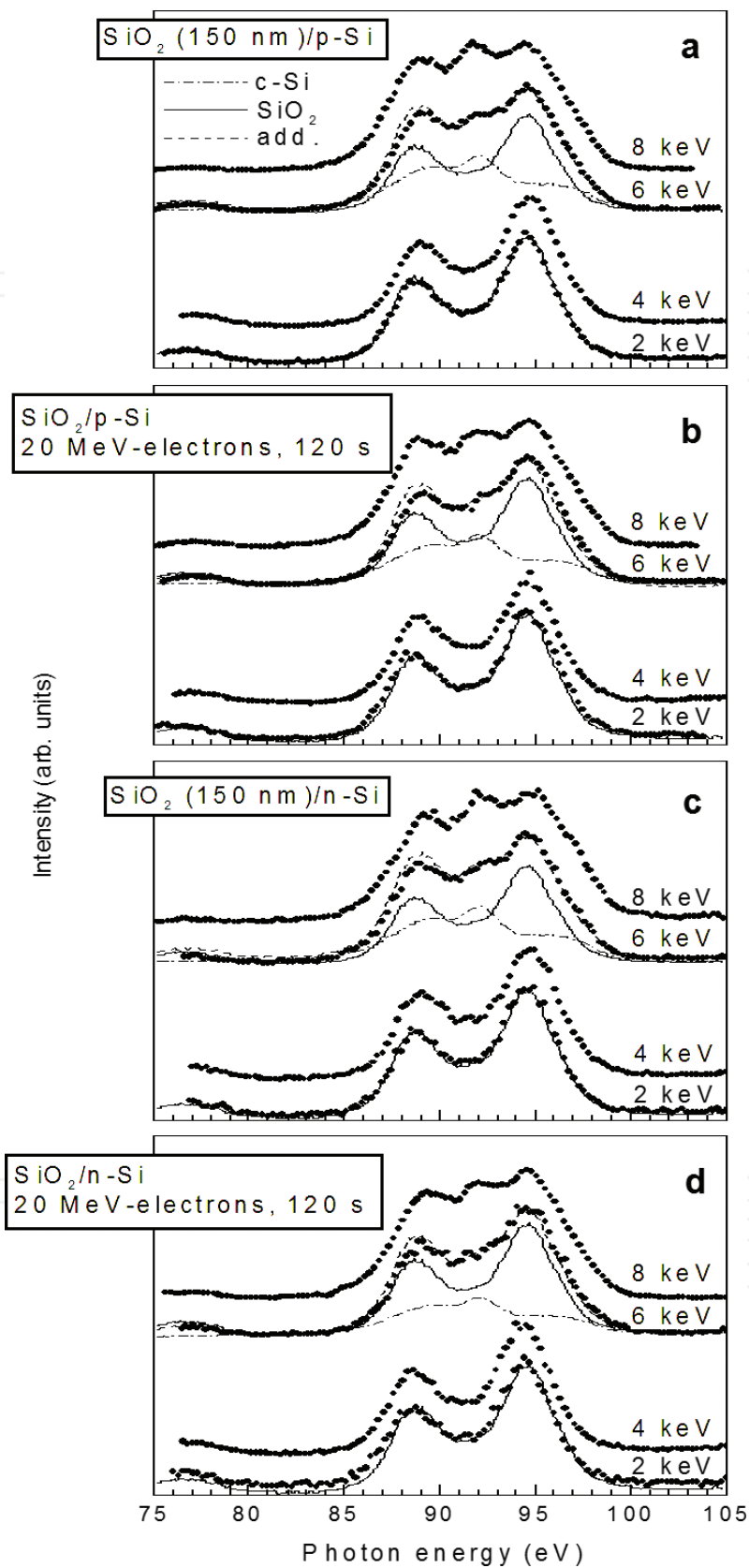


Figure 8. Si $L_{2,3}$ X-ray emission spectra measured at 2, 4, 6, and 8 keV for samples of the structure SiO_2 (150 nm)/p-Si and/n-Si as implanted (a) and (c) and after irradiation with 20 MeV electrons for 120 s (b) and (d), respectively.

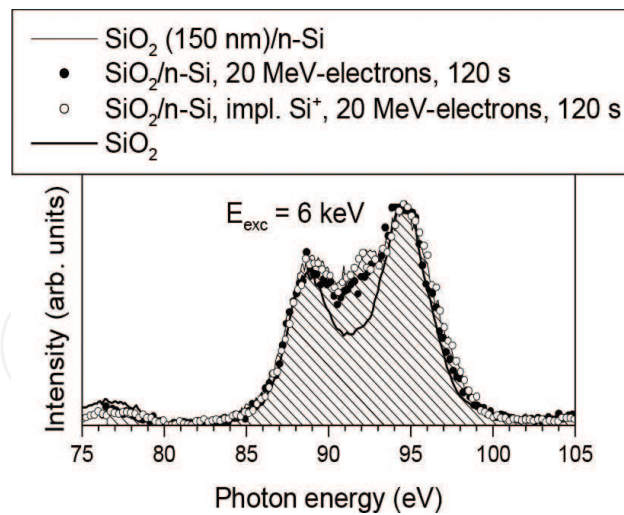


Figure 9. Si L_{2,3} X-ray emission spectra for SiO₂ (150 nm)/n-Si specimens as implanted (shaded region), after 20 MeV electron irradiation for 120 s (dots), and after 65 keV Si⁺ implantation and irradiation with electrons for 120 s (open symbols). The spectra were measured at an excitation energy of 6 keV. The spectrum of SiO₂ is presented as the solid line.

investigated in the present work. It was found that the effect of radiation-stimulated oxidation depends on the type of Si substrate. Our results demonstrate that the previous ion implantation blocks the oxidation process of the Si substrates, which takes place during MeV electron irradiation. This effect depends on the type of the silicon substrate, and it is more pronounced for samples prepared on n-type silicon substrates and it also depends on the post-oxidation treatment of the samples [6].

8. Si nanoclusters' generation in SiO₂ of ion-implanted Si-SiO₂ structures by MeV electron irradiation

SiO₂ surface roughness changes induced by high-energy electron irradiation of ion-implanted Si-SiO₂ structures are observed by atomic-force microscopy (AFM) measurements.

Here, amorphous SiO₂ transformation into crystalline Si is demonstrated. It is shown that silicon accumulation is observed and silicon nanocrystals are formed at the SiO₂ surface after high-energy electron irradiation. Silicon nanocrystals generated by MeV electron irradiation are observed in the SiO₂ matrix of Si-SiO₂ structures, implanted with different doses of silicon ions.

n-type CZ Si <100> wafers are cleaned and then oxidized in dry O₂ at 950°C to an oxide thickness of 20 nm. The oxide thickness is determined by the ellipsometry technique. After oxidation, the Si-SiO₂ samples are implanted through the oxide by 15 keV silicon ions with a dose of 1.5×10^{12} and 1.0×10^{16} cm⁻². The ion energy is chosen so as to produce maximum ion damage at the Si-SiO₂ interface. The implanted samples are simultaneously exposed to 20 MeV electrons perpendicular to the SiO₂ surface. Electron irradiation with a flux of 1.2×10^{15} el/cm² is carried out in a Microtron MT-25, in the Flerov Laboratory of Nuclear Reactions of JINR, Dubna, Russia.

Microscopic morphologies of SiO₂ surfaces of the implanted and irradiated Si-SiO₂ structures are observed by atomic force microscope (AFM). The AFM method is used as a measurement technique to study the changes observed in the dynamic properties of a vibrating tip that interacts with surface samples. This method allows one to resolve atomic-scale surface defects in ultra-high vacuum also. AFM images are taken over areas of 1 × 1 μm on the surface of the SiO₂-Si structures before and after the MeV electron irradiation of each of the samples.

Figure 10 presents AFM measurements of the implanted samples with doses of 10¹² cm⁻² Si ions (a), which is irradiated with 20 MeV electrons (b) and (c) for samples implanted with a

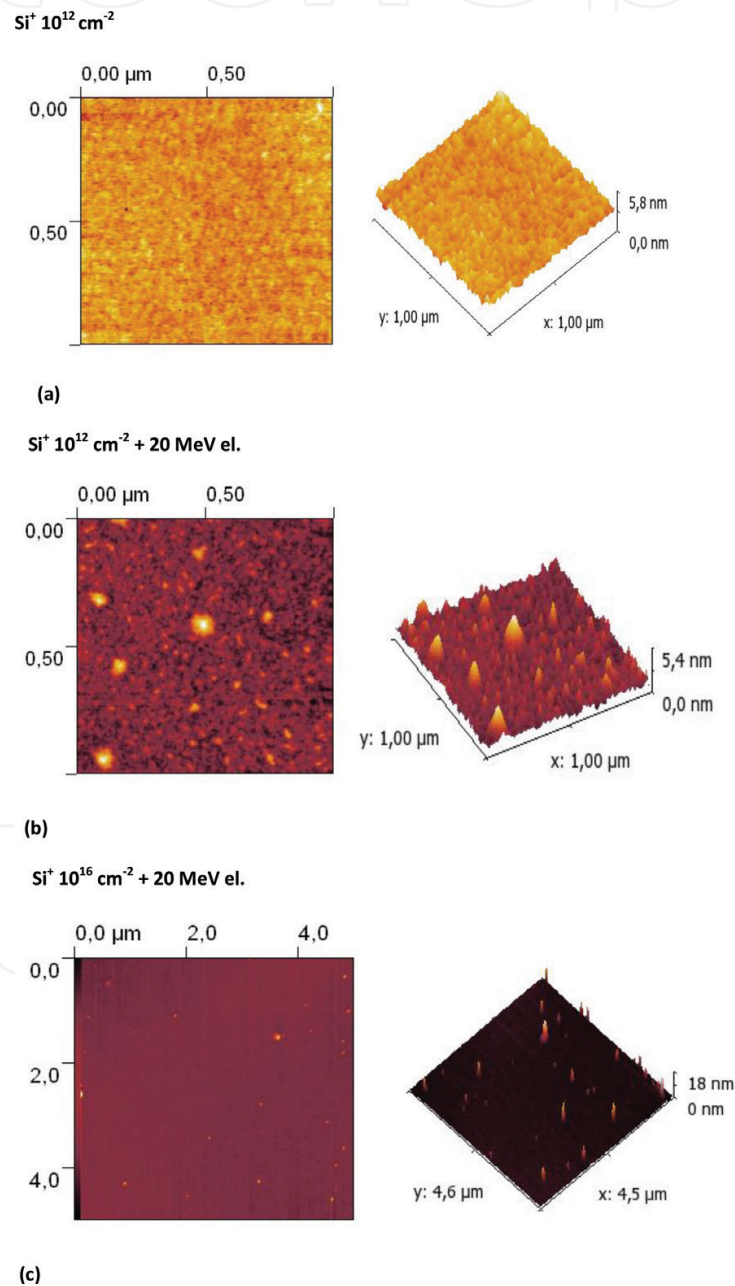


Figure 10. Surface morphology of silicon-implanted ions, Si-SiO₂ sample, before (a) and after electron irradiation (b) and (c).

dose of 10^{16}cm^{-2} Si ions and then irradiated with the same dose of MeV electrons. The AFM observation shows that the amorphous Si precipitations exist in the SiO₂ matrix after the ion implantation. Implanted Si atoms migrated and formed small precursor precipitations because implanted ions and implantation-induced damages were in some activated state. But it is obvious that these doses of 1.5×10^{12} and $1.0 \times 10^{16} \text{ cm}^{-2}$ for Si-implanted ions are not enough to create nanostructures in the oxide. Following 20 MeV electron irradiation (with a flux of $1.2 \times 10^{15} \text{ el/cm}^2$) generates new silicon nanostructures in SiO₂ with a different appearance and mode depending on the previous implanted dose.

We suppose that the radiation defects (created by MeV electron irradiation) appear as a source for Si nanostructure generation in the SiO₂. We assume that these nanostructures are silicon nanocrystals generated in SiO₂ by MeV electrons. AFM observation showed that the nanocrystal size is different depending on the dose of the previous implanted ions in SiO₂. The variation of the nanocrystal size can be related to the reduction of the oxygen ion concentration at the oxide surface. The nanocrystals are bigger for samples implanted with bigger doses ($1 \times 10^{16} \text{ cm}^{-2}$) but their number at cm^{-2} is lower as can be seen in **Figure 1(c)** and in **Table 1**. The parameters of silicon nanocrystals created by MeV electrons in the Si-SiO₂ samples previously implanted with different doses of silicon ions are presented in **Table 1**. Obviously, the mean silicon crystal high and the mean silicon crystal length are higher for the crystals created in the samples previously implanted with higher doses of (10^{16} cm^{-2}) silicon ions.

The ion implantation breaks many of the Si-O bonds and also may knock atoms from their sites. However, most of the atoms, silicon or oxygen, bond again shortly after being dislodged. In this way, one can explain the bigger size of the nanocrystals observed after electron irradiation in silicon-implanted samples (dose 10^{16} cm^{-2}) demonstrated in **Figure 9(c)**.

MeV electron irradiation effects of surface morphology of Si-SiO₂ structures implanted with different doses of silicon ions (doses of 1.5×10^{12} or $1.0 \times 10^{16} \text{ cm}^{-2}$) have been characterized by AFM observations. It has been demonstrated that MeV electrons (a flux of $1 \times 10^{15} \text{ cm}^{-2}$) created Si nanocrystals in SiO₂ films in both groups of silicon-implanted samples. A form and a density of the formed Si nanocrystals depend significantly on the previously implanted silicon ion dose. The SiO₂ surface morphology has shown that Si nanocrystals are created in SiO₂ films after electron irradiation only [7].

Silicon nanocrystals generated by MeV electron irradiation in silicon ion-implanted Si-SiO₂ structures are compared with those in the SiO₂ matrix of Si-SiO₂ structures, implanted with oxygen ions (with a dose of $1.5 \times 10^{12} \text{ cm}^{-2}$).

Sample	l_{mean} [nm]	h_{mean} [nm]	l_{max} [nm]	h_{max} [nm]
Si ⁺ 10^{12} + 20 MeV	50	2.3–4.2	50–124	4.2
Si ⁺ 10^{16} + 20 MeV	35	9–16	190	16

Table 1. Si crystal high and Si crystal length for the nanocrystals created by MeV electrons.

n-type Si <100> wafers are oxidized up to the oxide thickness of 20 nm. The Si-SiO₂ samples were implanted through the oxide by 15 keV Si⁺ or 10 keV O⁺ ions with a same dose of $1.5 \times 10^{12} \text{ cm}^{-2}$. The ion energy was chosen so as to produce maximum ion damage at the Si-SiO₂ interface. The implanted samples and non-implanted samples were simultaneously exposed to 20 MeV electrons perpendicular to the SiO₂ surface. Electron irradiation with a flux of $1.2 \times 10^{15} \text{ el/cm}^2$ is carried out in a Microtron MT-25 in the Flerov Laboratory of Nuclear Reactions of Joint Institute for Nuclear Research (FLNR, JINR) Dubna, Russia. The microscopic morphologies of reference sample SiO₂ surfaces, implanted or irradiated Si-SiO₂ structures were observed by the atomic force microscope (AFM) technique.

AFM images of the non-implanted sample before (a) and after 20 MeV electron irradiation (b) are demonstrated in **Figure 11**. Accumulation of nanostructures at the SiO₂ surfaces is observed only after MeV electron irradiation. Radiation defect creation by MeV electron acts as a source for Si nanostructures' generation in the SiO₂.

AFM images of Si- and O-implanted samples (a), and such samples irradiated by 20 MeV electrons (b), are presented in **Figures 10 and 11**, respectively. Energy (of 10–15 keV) and a dose (of $1.5 \times 10^{12} \text{ cm}^{-2}$) for the implanted ions are not sufficient to create nanostructures in the oxide. Structural modifications on the SiO₂ surface are observed after the ion implantation. 20 MeV electron irradiation (with a flux of $1.2 \times 10^{15} \text{ el/cm}^2$) generates a new silicon nanostructure in SiO₂ with a different appearance and mode. These nanostructures are silicon nanocrystals generated by MeV electrons in SiO₂. The nanocrystal sizes are different depending on the ions implanted in SiO₂.

Table 1 presents the lateral size and height of the silicon nanocrystals generated by MeV electrons in ion-implanted structures. The nanocrystal size depends on the implantation dose.

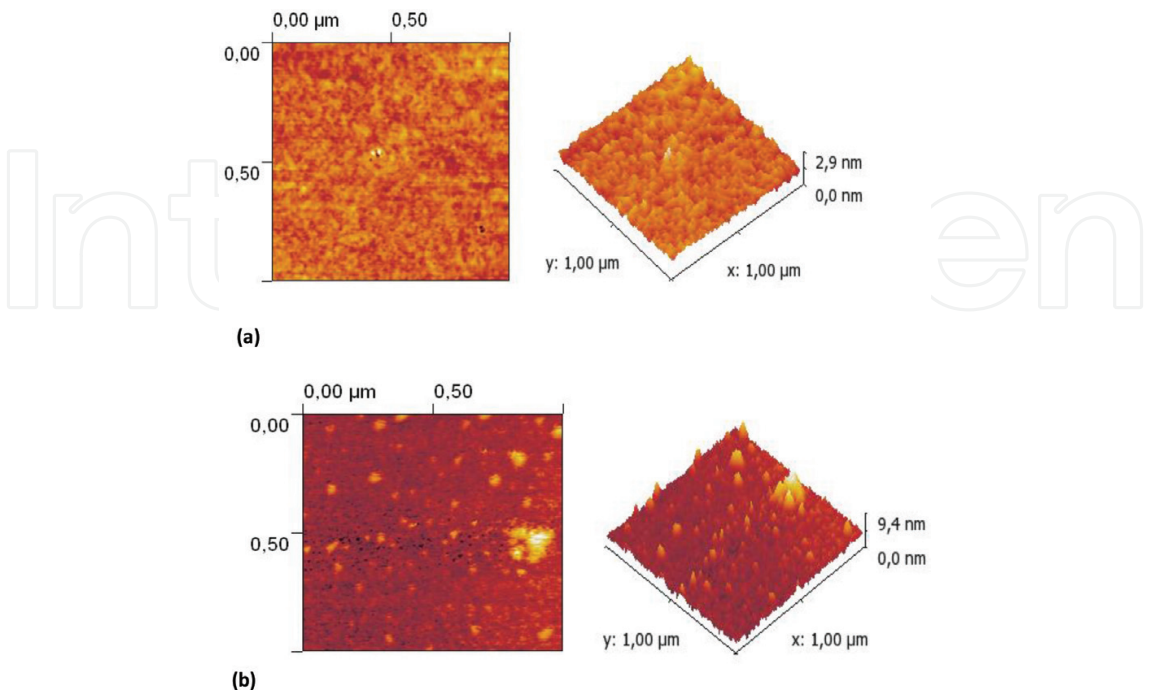


Figure 11. Surface morphology of Si-SiO₂ sample before (a) and after electron irradiation (b).

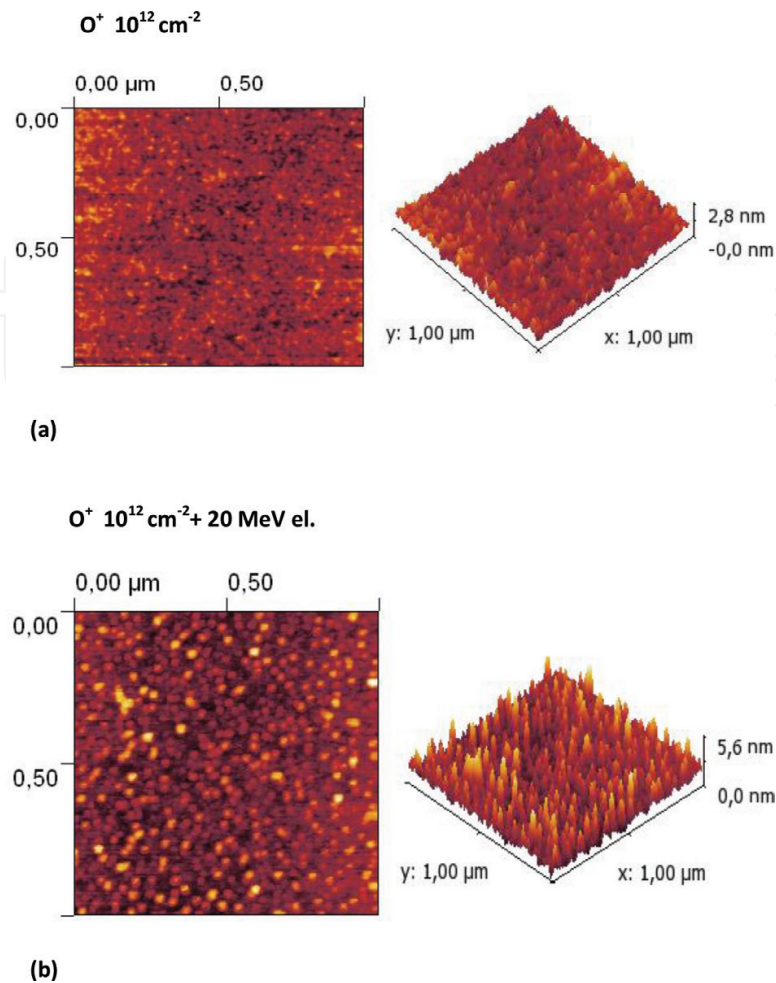


Figure 12. Si-SiO₂ sample implanted with O⁺ ions (dose of 10¹² cm⁻²) before (a) and after (b) MeV electron irradiation.

The nanocrystal size variation can be related to the reduction of the oxygen ion concentration at the SiO₂ oxide surface. The larger nanocrystals with lower densities are in silicon-implanted samples. The nanocrystals in oxygen-implanted samples (**Figure 12**) are narrower but with a higher density. The ion implantation rearranges the Si-O-Si groups in a different form. Many of the Si-O bonds break during the implantation. It also knocks down some of atoms from their sites. But, most of the atoms (after being dislodged) bond again shortly.

An insignificant decrease of the oxygen concentrations and slight increase of silicon concentrations are observed after high-energy MeV electron irradiation. The amorphous layer's thickness on the surface of the implanted Si-SiO₂ samples also increases after MeV electron irradiation. Accumulation of silicon at the SiO₂ surface after high-energy electron irradiation is one of the reasons for silicon nanocrystals' form. MeV electron irradiation breaks Si-O bonds and free oxygen is generated. As a result, radiation-stimulated motion through defects takes place.

The surface of the implanted Si-SiO₂ before and after high-energy electron irradiation is presented in **Figure 12**. The effects of MeV electron irradiation on the surface morphology of Si-SiO₂ structures (implanted with silicon or oxygen ions) are studied by AFM. After implantation, MeV electron irradiation generates additional radiation defects in the entire Si-SiO₂ structure. It is supposed that radiation-enhanced diffusion of oxygen takes place.

This can be the reason for the creation of Si nanocrystals in the SiO₂ oxide of the implanted samples. The shape and density of Si nanocrystals depend on the type of implanted ions. Si nanocrystals are created in SiO₂ of the implanted Si-SiO₂ structure after MeV electron irradiation only [8, 9].

Our investigation into the effect of the secondary MeV electron irradiation of pre-implanted silicon heterostructures shows a variety of processes depending on post-irradiation, its energy, and doses, as well as on the ion implantation parameters. In particular, MeV electron irradiation (which when carried out at room temperature) simulates two high-temperature processes (radiation-stimulated oxidation and radiation defects annealing) in silicon heterostructures.

Author details

Sonia B. Kaschieva^{1*} and Sergey N. Dmitriev²

*Address all correspondence to: kaschiev@issp.bas.bg

1 Institute of Solid State Physics, Bulgarian Academy of Sciences, Sofia, Bulgaria

2 Joint Institute for Nuclear Research, Dubna, Russia

References

- [1] S. Kaschieva, K. Stefanov, D. Karpusov. Electron irradiation of ion-implanted n-type Si-SiO₂ structures studied by DLTS. *Appl. Phys. A*. 66: 561 (1998).
- [2] S. Kaschieva, C. Angelov, S.N. Dmitriev. MeV electron irradiation of O⁺ or P⁺ implanted Si-SiO₂ structures. *J. Optoelectron. Adv. Mater.* 11(10): 150 (2009).
- [3] S. Kaschieva, C. Angelov, S.N. Dmitriev, G. Tsutsumanova. RBS investigation of ion implanted Si-SiO₂ structures irradiated with 20 MeV electrons, *Plasma Process. Polym.* 3: 233–236 (2006).
- [4] S. Kaschieva, S.N. Dmitriev. Radiation defects introduced by MeV electrons in argon implanted MOS structures. *Appl. Phys. A*. 94(2): 257–261 (2009).
- [5] S. Kaschieva, S. Alexanrdova. High-energy electron irradiation of ion implanted MOS structures with different oxide thickness. *Nucl. Instr. Meth. Phys. Res. B*. 174: 324 (2001).
- [6] S.N. Shamin, V.R. Galakhov, S. Kaschieva, S.N. Dmitriev, A.G. Belov. Soft X-ray emission spectroscopy of the SiO₂/Si structures irradiated with high-energy electrons. *J. Mater. Sci. Mater. Electron.* 14: 809 (2003).
- [7] S. Kaschieva, A. Gushterov, P. Gushterova, S.N. Dmitriev. Si nanoclusters generated in Si-SiO₂ structures implanted with different doses of Si ions. *J. Phys. Conf. Ser.* 223: 12031 (2010).

- [8] S. Kaschieva, A. Gushterov, C. Angelov, S.N. Dmitriev. Formation of Si nanocrystals in ion implanted Si-SiO₂ structures by MeV electrons. *J. Phys. Conf. Ser.* 356: 012005 (2012).
- [9] S. Kaschieva, A. Gushterov, T. Apostolova, S.N. Dmitriev. *Nanoclusters in SiO₂ of ion implanted Si-SiO₂ structures generated by MeV electron irradiation*. Proceedings of the VI International Conference, "Beam Technologies and Laser Application", (2010), p. 75.

IntechOpen

IntechOpen

